

# Three-Dimensional Quantum Percolation Studied by Level Statistics

Atsushi KANEKO and Tomi OHTSUKI

*Department of Physics, Sophia University, Kioi-cho 7-1, Chiyoda-ku, Tokyo 102-8554.*

Three-dimensional quantum percolation problems are studied by analyzing energy level statistics of electrons on maximally connected percolating clusters. The quantum percolation threshold  $p_q$ , which is larger than the classical percolation threshold  $p_c$ , becomes smaller when magnetic fields are applied, i.e.,  $p_q(B=0) > p_q(B \neq 0) > p_c$ . The critical exponents are found to be consistent with the recently obtained values of the Anderson model, supporting the conjecture that the quantum percolation is classified onto the same universality classes of the Anderson transition. Novel critical level statistics at the percolation threshold is also reported.

Studies of percolation [1] have been attracting much interest and a number of applications have been proposed due to its simplicity. One of its important applications is to the transport properties in three-dimensional (3D) solids. However, at low temperature, the classical percolation picture is insufficient and the quantum effects should be seriously taken into account; thus localization due to the quantum interference effect vs. percolation becomes a very interesting problem [2].

Even if a maximum cluster percolates through the system, the wave function may be localized and be unable to carry current. Thus the quantum percolation threshold  $p_q$  is generally larger than the geometrical classical percolation threshold  $p_c$ . At  $p_q$ , the localization length diverges and the wave function extends through the percolating cluster. It is often debated whether this transition is the same as the Anderson transition [3]. If this is true, the critical exponent  $\nu$  describing the divergence of the localization length in the quantum percolation problem would be the same as that in the Anderson transition, and the scaling theory of localization would be valid [4,5]. Then, a number of studies on Anderson transition [6,7] can be used to study quantum percolation problems. However, estimates of the critical exponent  $\nu$  often differ from that obtained in the Anderson tight binding model. For example, renormalization group analyses of the quantum percolation problem gave  $\nu = 2.1$  [8,9],  $\nu = 1.9 \pm 0.5$  [10], and  $\nu = 1.86 \pm 0.05$  [11], which are considerably larger than the recent estimate  $\nu = 1.57 \pm 0.02$  using the Anderson model [12,13], as analyzed by the transfer matrix method [14].

The transfer matrix method, which has been successfully used in the study of the Anderson tight binding model, however, cannot be applied to the quantum percolation problem. This is because there is always a finite probability that all bonds connecting one plane of cross section to the next are vanishing, so that the system breaks into disconnected pieces. To overcome this

difficulty, it was proposed [15] that a missing bond be replaced by a bond whose transfer energy is very small ( $\sim 10^{-5}$ ) compared to the transfer energy between the connected bonds. A network of percolating wires was also considered where the effect of the missing bonds was exactly taken into account to calculate the two-terminal conductance [16]. Though the percolation thresholds determined in the above studies are consistent with the analytical studies of quantum percolation by the Pade approximation [17,18], the above numerical study of conductance and an analytical one [19] suggest low values of  $\nu$  (0.73 and 0.38, respectively) compared to that in the Anderson model.

The analysis of energy levels is free from such geometrical problems. The Thouless number calculated from the energy levels in different boundary conditions gives a good estimate of the quantum percolation threshold in a three-dimensional system [20,21], but the exponent  $\nu$  is  $1.95 \pm 0.12$ , which is larger than the estimate in the Anderson model. Thus, the estimates of critical exponent are widely scattered. Even in 2D where all the states are believed to be Anderson-localized [4], some of the above studies indicate that there is a localization-delocalization transition [18,20].

Another method to extract information on the Anderson transition from eigenvalues is the finite-size scaling analysis of energy level spacing [22–29]. Berkovits and Avishai [30] applied this method and obtained reliable values of  $p_q$  and  $\nu$  in the quantum percolation problem. The obtained value of the exponent  $\nu = 1.35 \pm 0.1$  for the quantum percolation problem coincides with that estimated in the Anderson model by the energy level statistics [26],  $\nu = 1.45 \pm 0.1$ , though it is still slightly small compared to that estimated by the transfer matrix method for the Anderson tight binding model.

One of the most striking features of the Anderson transition is that it is classified onto a few universality classes according to the symmetry under the operation of time reversal. Therefore, to study the quantum percolation problem in relation to the Anderson transition, the sensitivity of  $p_q$  and  $\nu$  to the breaking of the time reversal symmetry (TRS) is a very important subject that needs to be investigated.

Here we study the energy level statistics of the quantum percolation model and discuss the effect of the breaking of TRS. To be specific, we restrict ourselves to the bond percolation problems. A peculiar form of the universal function of the level spacing distribution at the critical point, which is related to the sensitivity to the boundary conditions, is also reported.

To describe the 3D quantum bond percolation model, we consider the following simple Hamiltonian,

$$H = \sum_{\langle ij \rangle} (t_{ij} a_i^\dagger a_j + \text{h.c.}), \quad (1)$$

where  $\langle ij \rangle$  denotes the nearest neighbors. The transfer integral is defined as

$$t_{ij} = \begin{cases} \exp(-2\pi i \phi_{ij}) & (\text{for connected bond}) \\ 0 & (\text{for disconnected bond}) \end{cases}, \quad (2)$$

where the energy unit is the absolute value of the transfer energy between connected bonds. Bonds are randomly connected with probabilities  $p$ .  $\phi_{ij}$  is the Peierls phase due to magnetic fields. When all the Peierls phases are set to 0, the Hamiltonian is time reversal symmetric, and we call it the time reversal symmetric (TRS) model. When the phases are not vanishing, the Hamiltonian is generally not time reversal symmetric. We set  $-\pi < \phi_{ij} < \pi$  randomly, and call this situation non-TRS model hereafter. The underlying lattice is a three-dimensional cube of length  $L$  with periodic boundary conditions imposed.

For each realization of connected bonds, we first identify the maximally connected percolating cluster, and then we diagonalize the Hamiltonian corresponding to this cluster by Lanczos method. The calculation is performed for  $N$  different realizations of random bond configurations, where  $N = 580, 300, 175$  and  $110$  for sizes  $L^3 = 12^3, 15^3, 18^3$  and  $21^3$ , respectively. These parameters are chosen so that the number of eigenvalues for each system size exceeds  $10^6$ .

We analyze the eigenenergies in the region where the density of states is smooth (Fig. 1). In the actual simulation, we take  $|E| = 0.2 \sim 0.8$ . Energy spectra are then unfolded [31,32], and the distribution function  $P(s)$  of adjacent level spacings  $s$  is calculated, which is normalized as

$$\int_0^\infty ds P(s) = 1, \quad \int_0^\infty ds s P(s) = 1. \quad (3)$$

For a sufficiently large size, we expect the Poissonian behavior  $P_P(s) = \exp(-s)$  for localized states, while it should be the Wigner-Dyson type for extended states [33,31] where  $P_{\text{Wig}}(s) \propto s^\beta \exp(-A_\beta s^2)$  ( $\beta = 1$  in the presence of TRS and  $\beta = 2$ , otherwise). Varying the probability  $p$  and the size  $L$ , we extract the information of the quantum percolation transition.

Plots of  $P(s)$  as a function of the bond occupation probability for the TRS model and the non-TRS model ( $L = 21$ ) are displayed in Fig. 2. It is clearly seen that the expected crossover from a Poissonian behavior to that of Wigner-Dyson type is manifested as we increase the value of  $p$ .

In order to obtain the critical value of the probability  $p_q$  and the critical exponent for the divergence of the localization length  $\nu$ , we define  $I(s)$  and  $\Lambda(p, L)$  as [24]

$$I(s) = \int_0^s P(s') ds', \quad (4)$$

and

$$\Lambda(p, L) = \frac{\int_0^{s_0} I(s) ds - \int_0^{s_0} I_P(s) ds}{\int_0^{s_0} I_{\text{Wig}}(s) ds - \int_0^{s_0} I_P(s) ds}. \quad (5)$$

Here we set  $s_0 = 1.2$ . We also use other quantities to characterize the critical behavior of level statistics, [28] and have confirmed that the results of the transition points and the critical exponents are almost the same.

Denoting  $\xi(p)$  as the localization length or the correlation length which diverges as

$$\xi(p) \sim \frac{1}{|p - p_q|^\nu}, \quad (6)$$

this function is expected to behave as

$$\begin{aligned} \Lambda(p, L) &= f[L/\xi(p)] \\ &= a_0 + a_1 [L(p - p_q)^\nu]^{1/\nu} + \\ &\quad a_2 ([L(p - p_q)^\nu]^{1/\nu})^2 + \dots \end{aligned} \quad (7)$$

near the critical probability  $p_q$ .

In Fig. 3, we show  $\Lambda(p, L)$  as a function of  $p$  for different sample sizes  $L = 12, 15, 18$  and  $21$ . All curves cross at a single point. By fitting  $\Lambda(p, L)$  to eq.(7), we can estimate the critical exponent as well as  $p_q$ .

In Table I, we summarize our results of the  $\chi^2$  fit to eq.(7). Here, the error bars of raw data as well as the fitting parameters are estimated using the bootstrap method [13,12,34,35]. Sizes less than  $L = 9$  give an unreasonably large  $\chi^2$ , so we have excluded them.

The earlier result by Berkovits and Avishai [30] for the TRS model gives  $1.35 \pm 0.1$ , which is smaller than the transfer matrix result for the Anderson model,  $1.57 \pm 0.02$  [36]. Here we have considered two possibilities: (i) the effect of energy levels of small disconnected clusters, and (ii) the corrections to scaling due to small sizes.

Let us begin with the first possibility. Including the levels of small disconnected clusters [30], in principle, influences the results, since levels in the isolated clusters are not correlated with those in the percolating cluster, which destroys the level correlation. However, the results from all the energy levels (TRS(all)) almost coincide with those extracted from the information of the eigenenergies only for the states on the percolating cluster (TRS). This might be due to the fact that we are observing the region far from the classical percolation threshold  $p_c \approx 0.249$ , and most of the states belong to the percolating clusters. [37] We conclude that the possibility (i) is irrelevant, and thus discuss next possibility (ii).

The analysis by finite-size scaling of the level statistics tends to give smaller values [22,24,26,30] compared to that by the transfer matrix method combined with finite-size scaling [7,12]. It is possible that such discrepancies

arise from the small size of the system, where corrections to scaling are not negligible [38–40,13]. To investigate the corrections to scaling, we omit the data for smaller system sizes [41]. In the TRS model, excluding smaller system sizes tend to increase  $\nu$ , which saturates around  $\nu \approx 1.5$ , in agreement with the Anderson model.

Breaking the time reversal symmetry (non-TRS model) decreases the value of the transition point  $p_q$  [42]. This can be attributed to the destruction of the constructive quantum interference among the time-reversed paths, which supports the idea that this transition is indeed the Anderson transition. In the non-TRS model,  $\nu$  tends to increase by excluding smaller system sizes, but the fitting becomes unstable when only the data for  $L = 18$  and  $21$  are used. We conclude that the value of  $\nu$  in the non-TRS model is consistent with that of the Anderson model belonging to the unitary universality class [12] ( $\nu = 1.43 \pm 0.02$ ).

Now we focus our attention on the level statistics at the critical point  $p_q$ . In Fig. 4, we plot the distribution functions  $P(s)$  for the nearest-neighboring level spacing  $s$  at  $p_q$  for various system sizes. They seem to be independent of the sizes, but are different from that for the Anderson model with the periodic boundary condition (p.b.c.) and from that with the fixed boundary condition (f.b.c.). Recently, it was reported that the form of  $P(s)$  at the critical point changes with the change of boundary conditions [43]. The critical distribution function  $P(s)$  obtained in the present study lies between the two extreme cases. This is consistent with the fact that some of the bonds are missing at the edges of the system in the percolation problem, so even if we adopt the periodic boundary conditions, the model is effectively closer to the one with f.b.c. Here, we have plotted the results for the non-TRS model, but the same behavior is also observed in the TRS model.

In conclusion, we have analyzed the three-dimensional percolation problems by the finite-size scaling analysis for the energy levels. Breaking the time reversal symmetry lowers the quantum percolation threshold. Both the time reversal symmetric and non-symmetric models exhibit the critical exponent  $\nu$  consistent with the results of Anderson tight binding model. At the critical point, the energy level spacing distribution, which characterizes the level statistics, becomes size-independent, which differs from the one in the Anderson model with p.b.c. or f.b.c.

At present, we cannot clearly show that the TRS model and the non-TRS model belong to different universality classes. It took large-scale numerical effort to distinguish one universality class from the other even for the Anderson model [12], since highly accurate data of less than 0.2% relative error are required. This high accuracy is very difficult to achieve by level statistics for the quantum percolation problem. Much more numerical effort is necessary for this purpose.

The authors would like to thank Professors Y. Avishai and K. Slevin for useful comments.

- 
- [1] D. Stauffer and A. Aharony: *Introduction to Percolation Theory* (Taylor and Francis, London, 1994).
  - [2] B. Shapiro: in *Percolation Structures and Process*, ed. G. Deutscher *et al.* Ann. Isr. Phys. Soc. (1983) 367.
  - [3] P.W. Anderson: Phys. Rev. **109** (1958) 1492 .
  - [4] E. Abrahams, P.W. Anderson, D.C. Liciardello and T. V. Ramakrishnan: Phys. Rev. Lett. **42** (1979) 673.
  - [5] A. Kawabata: Prog. Theor. Phys. Suppl. **84** (1985) 16.
  - [6] P. A. Lee and T. V. Ramakrishnan: Revs. Mod. Phys. **57** (1985) 287 .
  - [7] B. Kramer and A. Mackinnon: Rep. Prog. Phys. **56** (1993) 1469.
  - [8] T. Odagaki and K.C. Chang: Phys. Rev. B **30** (1984) 1612.
  - [9] K.C. Chang and T. Odagaki: J. Phys. A **20** (1987) L1027.
  - [10] L. Root and J.L. Skinner: Phys. Rev. B **33** (1986) 7738.
  - [11] L. Root, J.D. Bauer and J.L. Skinner: Phys. Rev. B **37** (1988) 5518.
  - [12] K. Slevin and T. Ohtsuki: Phys. Rev. Lett. **78** (1997) 4083.
  - [13] K. Slevin and T. Ohtsuki: Phys. Rev. Lett. **82** (1999) 382.
  - [14] A. MacKinnon and B. Kramer: Phys. Rev. Lett. **47** (1981) 1546; Z. Phys. B **53** (1983) 1.
  - [15] C.M. Soukoulis, Q. Li and G.S. Grest: Phys. Rev. B **45** (1992) 7724.
  - [16] Y. Avishai and J.M. Luck: Phys. Rev. B **45** (1992) 1074.
  - [17] Y. Shapir, A. Aharony and A.B. Harris: Phys. Rev. Lett. **49** (1982) 486.
  - [18] Y. Meir, A. Aharony and A.B. Harris: Europhys. Lett. **10** (1989) 275.
  - [19] I. Chang *et al.*: Phys. Rev. Lett. **74** (1995) 2094.
  - [20] Th. Koslowski and W. von Niessen: Phys. Rev. B **42** (1990) 10342.
  - [21] Th. Koslowski and W. von Niessen: Phys. Rev. B **44** (1991) 9926.
  - [22] B.I. Shklovskii, B. Shapiro, B.R. Sears, P. Lambrianides and H.B. Shore: Phys. Rev. **B47** (1993) 11487.
  - [23] Y. Ono and T. Ohtsuki: J. Phys. Soc. Jpn. **62** (1993) 3813.
  - [24] E. Hofstetter and M. Schreiber: Phys. Rev. **B48** (1993) 16979 ; **B49** (1994) 14726.
  - [25] S.N. Evangelou: Phys. Rev. **B49** (1994) 16805.
  - [26] I. Kh. Zharekeshev and B. Kramer: Jpn. J. Appl. Phys. **34** (1995) 4361; Phys. Rev. **B51** (1995) 17239; Phys. Rev. Lett. **79** (1997) 717.
  - [27] M. Batsch, L. Schweitzer, I. Kh. Zharekeshev and B. Kramer: Phys. Rev. Lett. **77** (1996) 1552 .
  - [28] L. Schweitzer and I. Kh. Zharekeshev: J. Phys. Cond. Matt. **9** (1997) L377.
  - [29] T. Kawarabayashi, T. Ohtsuki, K. Slevin and Y. Ono: Phys. Rev. Lett. **77** (1996) 3593.
  - [30] R. Berkovits and Y. Avishai: Phys. Rev. B **53**

- (1996)16125 .
- [31] M.L. Mehta: *Random Matrices* 2nd Edition (Academic Press, San Diego, 1991).
  - [32] Y. Ono, H. Kuwano, K. Slevin, T. Ohtsuki and B. Kramer: J. Phys. Soc. Jpn. **62** (1993) 2762.
  - [33] F.J. Dyson and M.L. Mehta: J. Math. Phys. **4** (1963) 701 .
  - [34] Ch. 15, *Numerical Recipes in Fortran*, W. Press, B. Flannery and S. Teukolsky, (Cambridge Univ. Press, Cambridge, 1992).
  - [35] Chs. 4-5 *Bootstrap Methods and their Application*, A. C. Davison and D. V. Hinkley, (Cambridge Univ. Press, Cambridge, 1997).
  - [36] Most literature use a standard deviation for the error bar of the exponent, but twice the standard deviation (95% confidence interval) was used in Slevin and Ohtsuki. [12,13] In order to avoid confusion, we cite the values by them with the error bar of single standard deviation.
  - [37] Y. Avishai: private communication.
  - [38] B. Huckestein: Phys. Rev. Lett. **72** (1994) 1080.
  - [39] Z. Wang, B. Jovanovic and D.-H. Lee: Phys. Rev. Lett. **77** (1996) 4426 .
  - [40] D.G. Polyakov: Phys. Rev. Lett. **81** (1998) 4696.
  - [41] T. Kawarabayashi, B. Kramer and T. Ohtsuki : Phys. Rev. **B57** (1998) 11842.
  - [42] Y. Meir, A. Aharony and A. Harris: Phys. Rev. Lett. **56** (1986) 976. In this reference, uniform magnetic fields are applied and a cyclotron motion is present, while in our random phase model, such motion is absent and the shift of  $p_q$  is purely from the breaking of TRS.
  - [43] D. Braun, G. Montambaux and M. Pascaud: Phys. Rev. Lett. **81** (1998) 1062.

FIG. 1. Normalized density of states of the quantum percolation problem for the non-TRS model. The solid line is for the maximally connected cluster, while the dashed line corresponds to all the energy levels including small clusters.

FIG. 2. Level spacing distribution  $P(s)$  for the TRS model (a) and the non-TRS model(b) for  $L = 21$ . With an increase in  $p$ , the transition from a Poisson distribution to that of Gaussian orthogonal ensemble is seen in Fig. 2(a), while the transition from a Poisson distribution to that of Gaussian unitary ensemble is seen in Fig. 2(b).

FIG. 3.  $\Lambda(p, L)$  as a function of  $p$  for different sample sizes for the TRS model (a) and the non-TRS model(b) obtained from the energy of the percolating cluster. Energy range is  $|E| = 0.2 \sim 0.8$ . At  $p_q$ , all curves cross at a point where  $\Lambda(p, L)$  becomes scale-independent. Bars around the data points indicate error bars estimated by the bootstrap method, and the curves are the results of the fit to eq.(7). Insets are the scaling plots.

FIG. 4. Critical level spacing distribution for the non-TRS model, which shows intermediate behavior between that of Anderson model with the p.b.c. (solid line) and those with f.b.c. (dashed line).

TABLE I. The  $\chi^2$  fitting of critical point  $p_q$  and critical exponent  $\nu$  with their standard deviations. The values of the TRS model and the non-TRS model are only for percolating cluster, while TRS (all) is obtained from all energy levels. TRS (all,BA) is the result reported by reported Berkovits and Avishai [30].

system	size	$p_q$	$\nu$
TRS (all,BA)	$L = 7, 9, 11, 13, 15$	$0.33 \pm .01$	$1.35 \pm .10$
TRS (all)	$L = 12, 15, 18, 21$	$0.321 \pm .001$	$1.48 \pm .10$
TRS	$L = 12, 15, 18, 21$	$0.324 \pm .001$	$1.46 \pm .09$
TRS	$L = 15, 18, 21$	$0.323 \pm .001$	$1.55 \pm .15$
TRS	$L = 18, 21$	$0.327 \pm .002$	$1.50 \pm .28$
non-TRS	$L = 12, 15, 18, 21$	$0.309 \pm .001$	$1.24 \pm .08$
non-TRS	$L = 15, 18, 21$	$0.308 \pm .001$	$1.44 \pm .16$

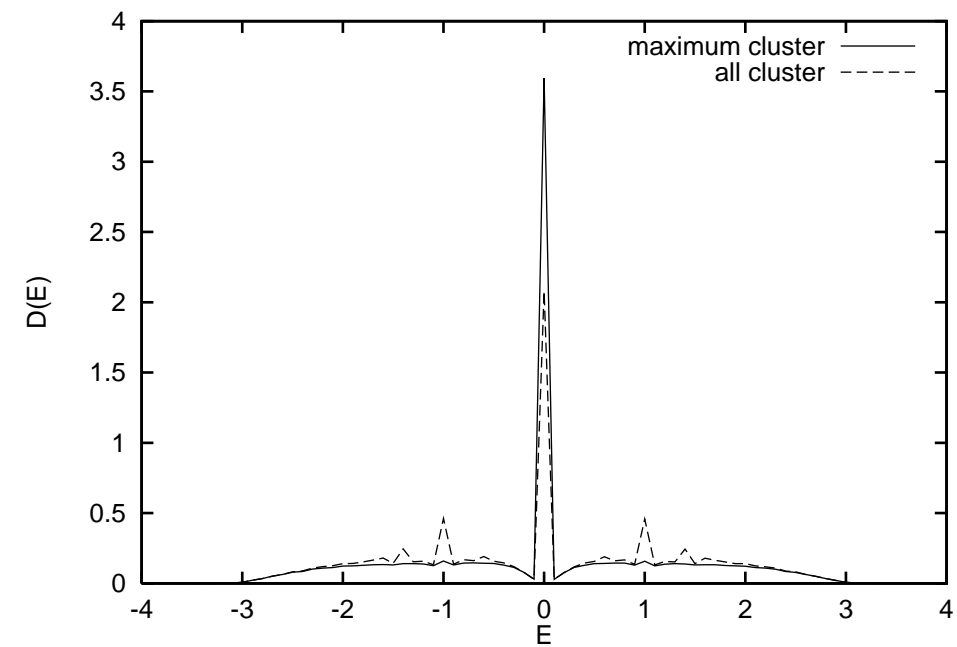


Fig. 1

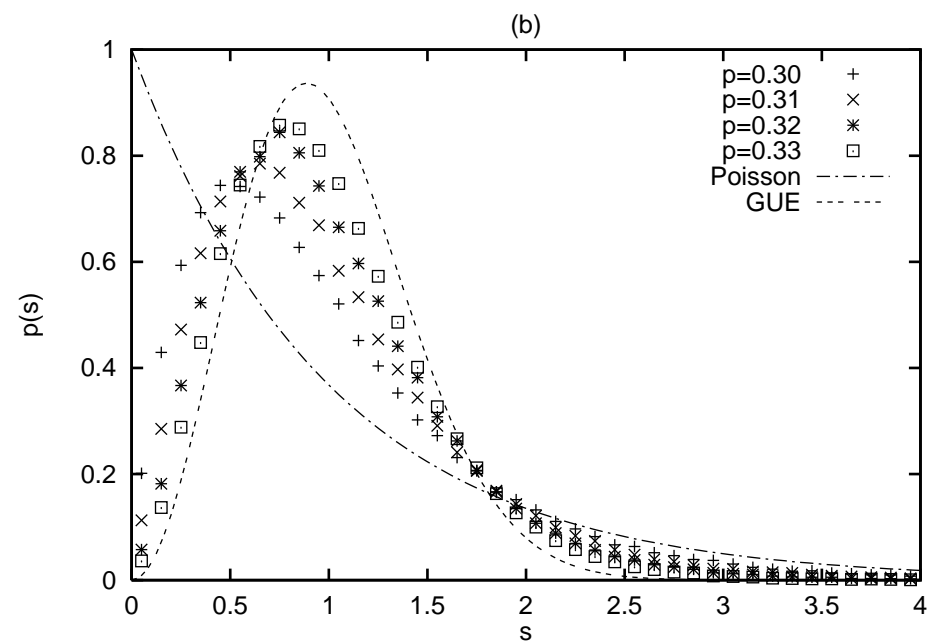
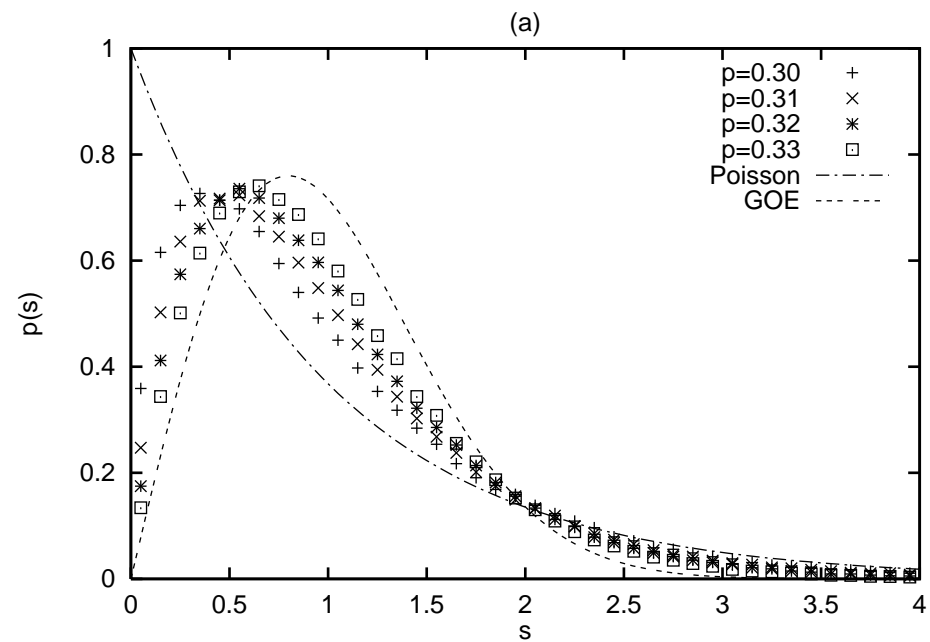


Fig. 2

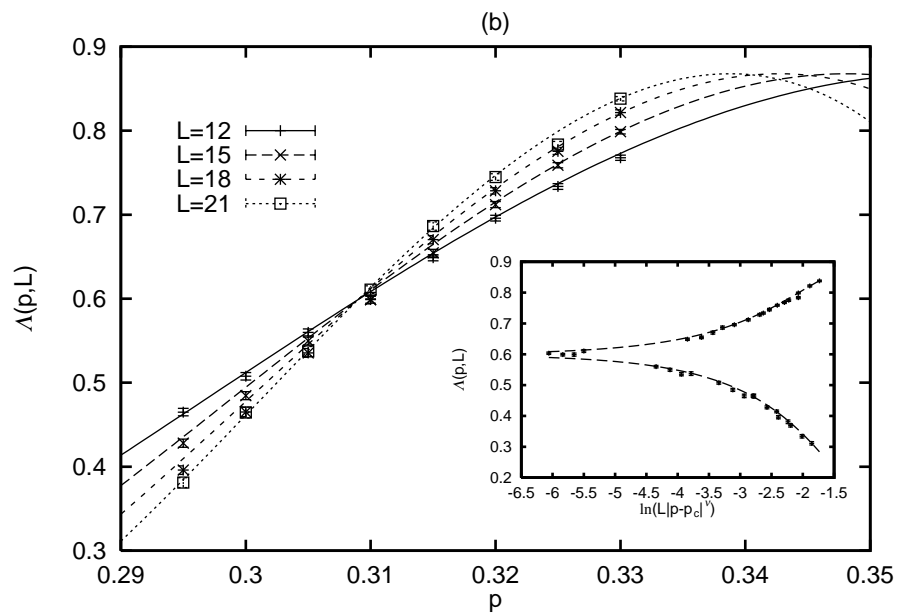
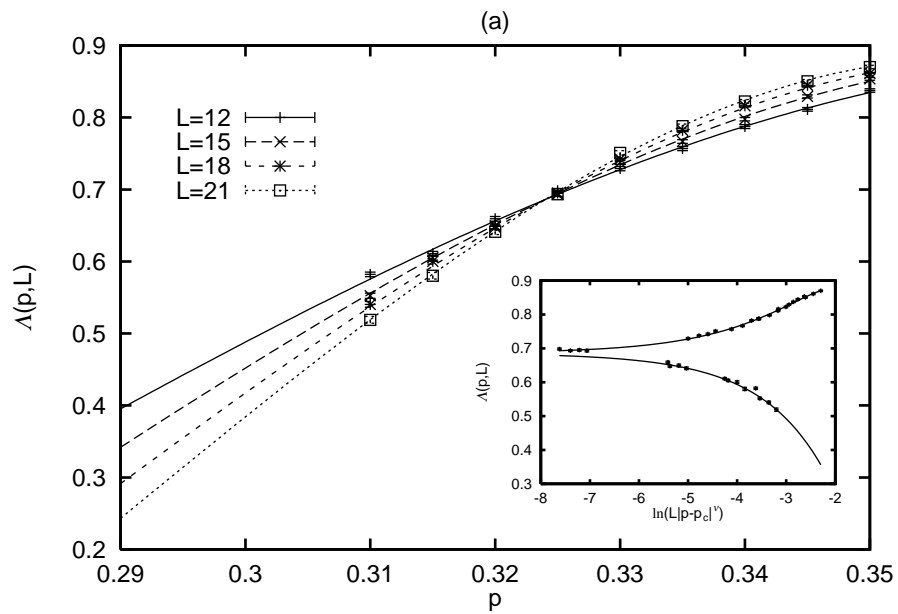


Fig. 3

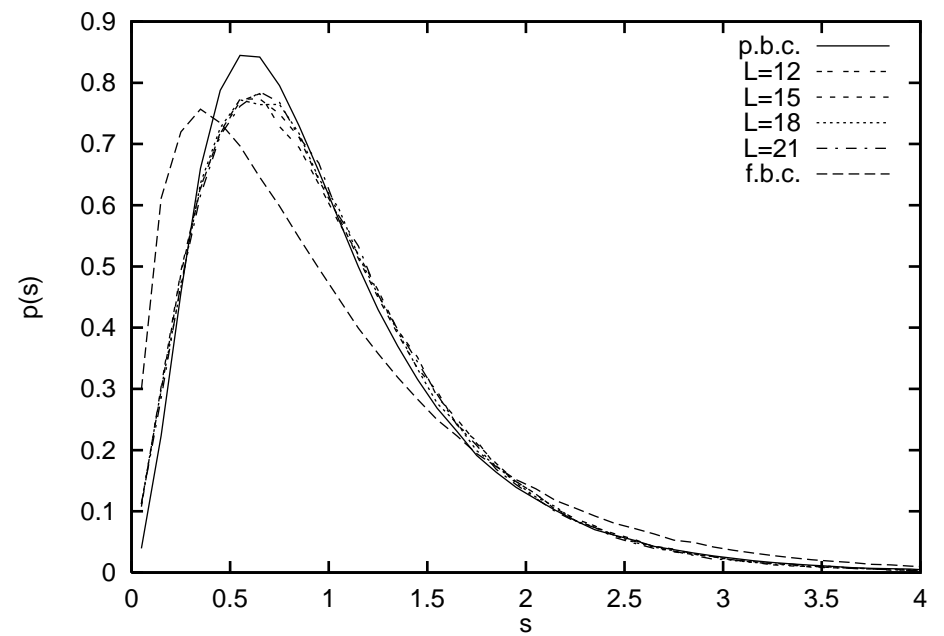


Fig. 4